ISSN 1674-1056
http://cpb.iphy.ac.cn
http://iopscience.iop.org/cpb
中国物理 B
Chinese Physics
中国物理
Chinese Physics B

Effect of defects properties on InP-based high electron mobility transistors

Shu-Xiang Sun(孙树祥), Ming-Ming Chang(常明铭), Meng-Ke Li(李梦珂), Liu-Hong Ma(马刘红), Ying-Hui Zhong(钟英辉), Yu-Xiao Li(李玉晓), Peng Ding(丁芃), Zhi Jin(金智), Zhi-Chao Wei(魏志超)

Citation: Chin. Phys. B . 2019, 28(7): 078501. **doi:** 10.1088/1674-1056/28/7/078501
Journal homepage: http://cpb.iphy.ac.cn; http://iopscience.iop.org/cpb

What follows is a list of articles you may be interested in

Dark count rate and band to band tunneling optimization for single photon avalanche diode topologies

Taha Haddadifam, Mohammad Azim Karami
Chin. Phys. B . 2019, 28(6): 068502. **doi:** 10.1088/1674-1056/28/6/068502

Modeling electric field of power metal-oxide-semiconductor field-effect transistor with dielectric trench based on Schwarz-Christoffel transformation

Zhi-Gang Wang(汪志刚), Tao Liao(廖涛), Ya-Nan Wang(王亚南)
Chin. Phys. B . 2019, 28(5): 058503. **doi:** 10.1088/1674-1056/28/5/058503

Optimization of ambipolar current and analog/RF performance for T-shaped tunnel field-effect transistor with gate dielectric spacer

Ru Han(韩茹), Hai-Chao Zhang(张海潮), Dang-Hui Wang(王党辉), Cui Li(李翠)
Chin. Phys. B . 2019, 28(1): 018505. **doi:** 10.1088/1674-1056/28/1/018505

Analysis of tail bits generation of multilevel storage in resistive switching memory

Jing Liu(刘璟), Xiaoxin Xu(许晓欣), Chuanbing Chen(陈传兵), Tiancheng Gong(龚天成), Zhaoan Yu(余兆安), Qing Luo(罗庆), Peng Yuan(袁鹏), Danian Dong(董大年), Qi Liu(刘琦), Shibing Long(龙世兵), Hangbing Lv(吕杭炳), Ming Liu(刘明)
Chin. Phys. B . 2018, 27(11): 118501. **doi:** 10.1088/1674-1056/27/11/118501

A snapback-free TOL-RC-LIGBT with vertical P-collector and N-buffer design

Weizhong Chen(陈伟中), Yao Huang(黄垚), Lijun He(贺利军), Zhengsheng Han(韩郑生), Yi Huang(黄义)
Chin. Phys. B . 2018, 27(8): 088501. **doi:** 10.1088/1674-1056/27/8/088501

Effect of defects properties on InP-based high electron mobility transistors*

Shu-Xiang Sun(孙树祥)[1,†], Ming-Ming Chang(常明铭)[1,†], Meng-Ke Li(李梦珂)[1], Liu-Hong Ma(马刘红)[1], Ying-Hui Zhong(钟英辉)[1,‡], Yu-Xiao Li(李玉晓)[1], Peng Ding(丁芃)[2], Zhi Jin(金智)[2], and Zhi-Chao Wei(魏志超)[3]

[1] *School of Physics and Engineering, Zhengzhou University, Zhengzhou* 450001, *China*
[2] *Institute of Microelectronics, Chinese Academy of Sciences, Beijing* 100029, *China*
[3] *China Academy of Space Technology, Beijing* 100086, *China*

(Received 14 March 2019; revised manuscript received 17 April 2019; published online 21 May 2019)

The performance damage mechanism of InP-based high electron mobility transistors (HEMTs) after proton irradiation has been investigated comprehensively through induced defects. The effects of the defect type, defect energy level with respect to conduction band E_T, and defect concentration on the transfer and output characteristics of the device are discussed based on hydrodynamic model and Shockley–Read–Hall recombination model. The results indicate that only acceptor-like defects have a significant influence on device operation. Meanwhile, as defect energy level E_T shifts away from conduction band, the drain current decreases gradually and finally reaches a saturation value with E_T above 0.5 eV. This can be attributed to the fact that at sufficient deep level, acceptor-type defects could not be ionized any more. Additionally, the drain current and transconductance degrade more severely with larger acceptor concentration. These changes of the electrical characteristics with proton radiation could be accounted for by the electron density reduction in the channel region from induced acceptor-like defects.

Keywords: InP-based high electron mobility transistor, proton radiation, defects properties, output and transfer characteristics

PACS: 85.30.De, 73.61.Ey, 14.20.Dh **DOI:** 10.1088/1674-1056/28/7/078501

1. Introduction

In the past few decades, with the development of advanced micro/nano-fabrication technologies or novel structures,[1–3] III–V compound semiconductor devices have attracted considerable attention.[4–7] Among them, the great progress of InP-based high electron mobility transistors (HEMTs) has been made; for example, the current gain cut-off frequency f_T and maximum oscillation frequency f_{max} have been reported to be above 700 GHz and 1 THz.[8,9] Therefore, InP-based HEMTs are potentially excellent candidates for various high speed circuits, millimeter wave systems, and even terahertz applications,[10–12] such as national defense, aerospace, and satellite radar.

In the environment of space, various high-energy particles and rays will damage the electronic devices and result in performance degradation of devices and even abnormality of electronic systems.[13,14] The main sources of energetic particles in space environments are protons and electrons. However, the proton mass is about 1836 times larger than that of electron, which means that more serious radiation damage could be induced by protons. Therefore, it is very important to study the effect of proton irradiation on InP-based HEMTs used in space environment.

Admittedly, some exploratory studies have yet been reported to be aimed at proton irradiation effect on HEMT devices,[15–17] most of which have focused on the performance degradation of devices caused by different proton fluences and proton energies. Much less has been done to study the effects on the defects properties induced by proton irradiation, such as the type of defects and the defect energy level. Under appropriate conductions, the defects induced by proton irradiation will interact with other impurity atoms and vacancies, forming more complex defects. Consequently, the deep defect level will be introduced into the forbidden band of materials,[18,19] which will reduce the carrier concentration and degenerate the device of performance through changing the Fermi energy level by electrical compensation. Therefore, it is very indispensable to make a clear understanding of the irradiation damage mechanism of InP-based HEMTs by defects properties.

In this paper, the effect of defects properties on InP-based HEMTs is investigated by hydrodynamic model and Shockley–Read–Hall recombination model, including the defect type, defect energy level, and defect concentration. The results will provide an effective analytical approach and reliable theoretical guidance for anti-radiation of InP-based HEMT.

*Project supported by the National Natural Science Foundation of China (Grant Nos. 11775191, 61404115, 61434006, and 11475256), the Development Fund for Outstanding Young Teachers in Zhengzhou University of China (Grant No. 1521317004), and the Doctoral Student Overseas Study Program of Zhengzhou University, China.

†These authors contributed equally to this work.
‡Corresponding author. E-mail: zhongyinghui@zzu.edu.cn

© 2019 Chinese Physical Society and IOP Publishing Ltd

2. Device structure and numerical methods

Figure 1 shows a schematic cross-section of InP-based HEMTs. The epitaxial structure from bottom to top consists of an $In_{0.52}Al_{0.48}As$ buffer, an $In_{0.53}Ga_{0.47}As$ channel, $In_{0.52}Al_{0.48}As$ spacer layer, a Si-doped plane which provides two-dimensional electron gas (2DEG), a 12 nm thick unstrained $In_{0.52}Al_{0.48}As$ Schottky barrier layer, and a heavily Si-doped doping InGaAs cap layer. All InAlAs layers are lattice matched with the InP substrate. Source and drain ohmic contacts are spaced 2.4 μm apart with 0.1 μm T-gate being located at the center of gate-recess region. The detailed fabrication process has been described in our previous work.[20,21]

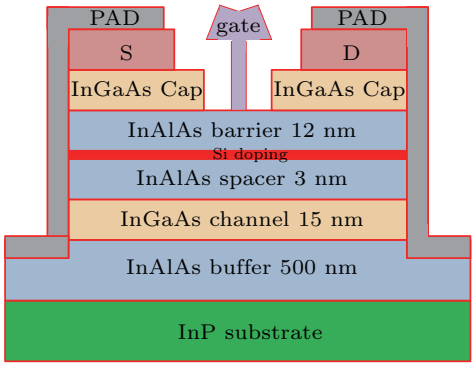


Fig. 1. Schematic cross-section of the InP-based HEMT.

To investigate the effect of proton radiation on the electrical characteristics of InP-based HEMT, the numerical simulation method has been used.[10] For devices with heterostructure, electrons can acquire very high energy and get into non-equilibrium transport condition, and therefore electron velocity can be much greater than their steady state value. Coincidentally, hydrodynamic transport model depicts charge transport properties through Poisson equation, continuity equation, and energy conservation equation, which can thus precisely describe many non-equilibrium conditions such as quasi-ballistic transport in thin regions and velocity overshoot effect in depleted regions. Moreover, the induced vacancies by displacement effect after proton irradiation are considered self-consistently through solving Poisson and current continuity equations and energy conservation equations as follows:[8,22]

$$\nabla \cdot \varepsilon \nabla \phi = -q\left[p - n + N_{\mathrm{D}} - N_{\mathrm{A}}\right] - \rho_{\mathrm{trap}}, \quad (1)$$

$$J_{\mathrm{n}} = q\mu_{\mathrm{n}}\left(n\nabla E_{\mathrm{C}} + kT_{\mathrm{n}}\nabla n + kn\nabla T_{\mathrm{n}} - 1.5nkT_{\mathrm{n}}\nabla \ln m_{\mathrm{n}}\right), \quad (2)$$

$$\nabla S_{\mathrm{n}} = J_{\mathrm{n}} \cdot \nabla E_{\mathrm{C}} - n\frac{\partial w_{\mathrm{n}}}{\partial t} - n\frac{w_{\mathrm{n}} - w_0}{\tau_{\mathrm{e}}}, \quad (3)$$

where ε is the electrical permittivity, φ is the electrostatic potential, n and p are the electron and hole densities, N_{D} and N_{A} are the ionized donor and acceptor concentration, ρ_{trap} is the charge density contributed by defects, E_{C} is the conduction band energy, T_{n} is the electron temperature, m_{n} is the electron effective masses, S_{n} is the energy flux, and τ_{e} is the energy relaxation time. To explain the single defect level in the band gap, the Shockley–Read–Hall model is adopted as follows:[23,24]

$$R_{\mathrm{SRH}} = \frac{np - n_{\mathrm{ie}}^2}{\tau_{\mathrm{p}}\left(n + n_{\mathrm{ie}}\exp\dfrac{E_{\mathrm{T}} - E_{\mathrm{i}}}{kT}\right) + \tau_{\mathrm{n}}\left(p + n_{\mathrm{ie}}\exp\dfrac{E_{\mathrm{i}} - E_{\mathrm{T}}}{kT}\right)}, \quad (4)$$

where n_{ie} is the effective intrinsic density, and E_{T} is the defect level with respect to conduction band.

Several crucial physical effects are also taken into account in the simulation, including doping and high field dependent mobility degradation models, impact ionization model, quantum effect model, and Auger and radiative recombination models.[25,26] The parameters of $In_{0.52}Al_{0.48}As$ and $In_{0.53}Ga_{0.47}As$ materials are obtained by liner interpolation from the parameters of AlAs, GaAs, and InAs. The temperature is 300 K by default in the simulations. The Newton method is adopted to calculate the equations of the physical models. Additional information about the models and parameters is described in our previous work.[27,28]

3. Results and discussion

It is well-known that carriers are mainly distributed and gathered around InAlAs/InGaAs hetero-junction in InP-based HEMTs, which thus determines almost all of the device characteristics, including channel current, transconductance, and so on. Therefore, the number of induced vacancies in InAlAs barrier and InGaAs channel layer is calculated with proton energy varying from 50 keV to 200 keV, as shown in Fig. 2. The number of induced vacancies around hetero-junction increases firstly and decreases subsequently, which reaches the largest value at 75 keV. With the increase of proton energy, the proton injection depth will increase gradually, and eventually protons pass through the material layers with only a small amount of vacancies generated in hetero-junction region.

The induced vacancies may influence devices by acting as acceptor-like or donor-like defects, which is closely related with their concentration and energy level. Among Al, As, Ga, and In vacancies induced by proton radiation, the As vacancy will become acceptor-like defects, while Ga and In vacancies will conduct as donor-like defects.[29] To estimate their impacts on InP-based HEMTs, the output channel current I_{DS} with gate-source voltage V_{GS} of 0 V and transfer characteristics with drain–source voltage V_{DS} of 1.5 V are investigated before and after proton irradiation at fluence of 1×10^{12} cm^{-2}, as shown in Fig. 3. The output channel current and transfer characteristics are degraded gradually only with acceptor-like defect; however, donor-like defects have no effect on device performance because the negatively charged As acceptor defects induced by proton irradiation capture the free electrons and thus result in performance degradation of InP-based HEMTs.

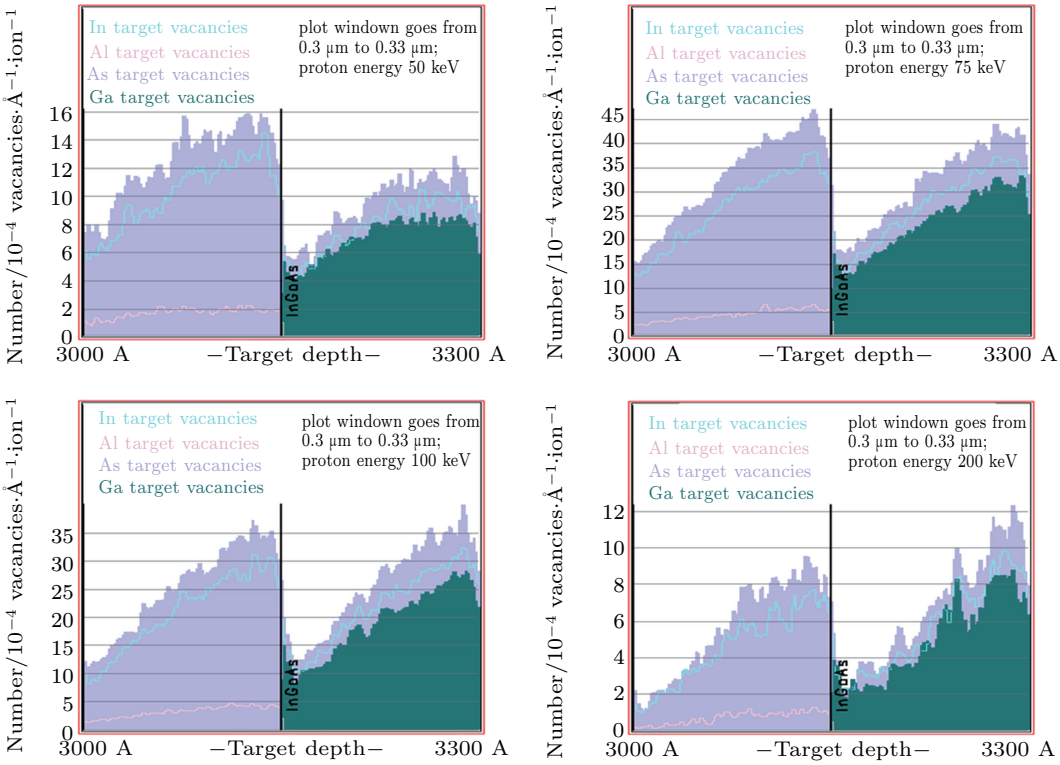


Fig. 2. The number of vacancy defects in hetero-junction material layers induced by proton radiation with different energies.

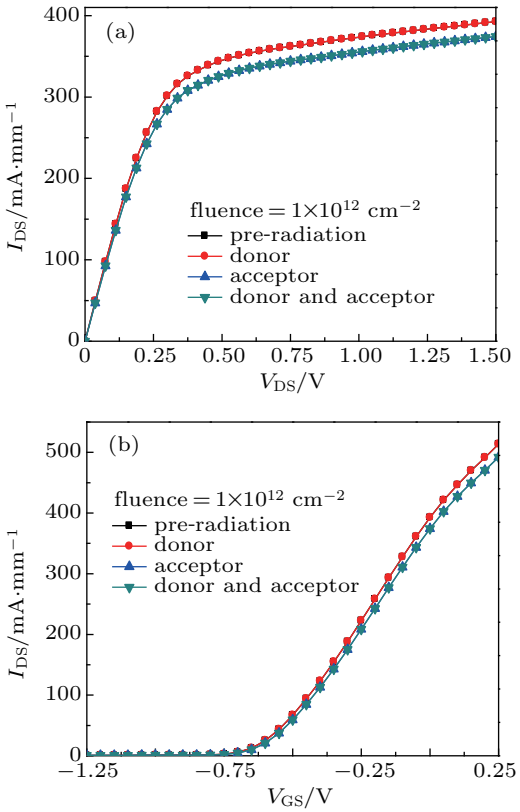


Fig. 3. Output channel current and transfer characteristics with donor and acceptor defects. (a) Output channel current; (b) transfer characteristics.

The energy level in band-gap of material is another important factor of defects, which may affect the degradation degree of device performance. Figures 4 and 5 show the transfer characteristics and output channel current versus defect energy level with respect to conduction band E_T with concentration fixed at 1×10^{12} cm^{-2}. With the increase of the energy level distance from conduction band, the drain current decreases and saturates at an energy level distance of 0.5 eV, which is mainly due to the fact that defects recombination rate rises with the increase of the defects energy level. The defects recombination rate can be written as[24]

$$R_{\mathrm{SRH}} = p \times \left[\tau_{\mathrm{p}}\left[1 + \frac{n_1}{N_{\mathrm{C}}\exp(-\eta_{\mathrm{n}})}\right]\right]^{-1},$$

where $n_1 = n_{\mathrm{i,eff}}\exp\left(E_{\mathrm{Trap}}/kT\right)$. Therefore, the defects recombination rate will be increased as the defects energy level increases. Namely, the fewest electrons are captured at the 0 eV defect level, whereas the most electrons are captured at

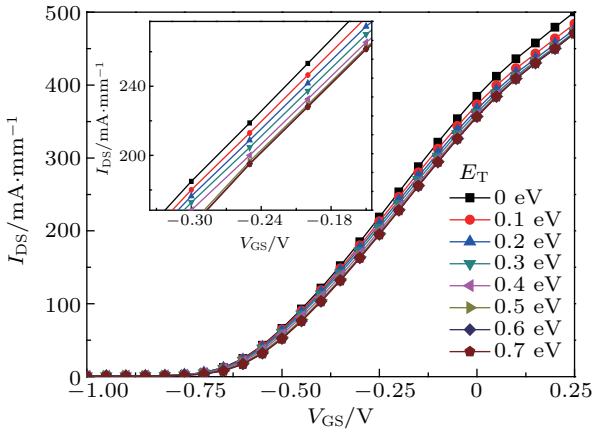


Fig. 4. The effect of E_T on transfer characteristics.

0.7 eV, as shown in Fig. 6. Moreover, the drain current has a small change over the 0.5 eV defect energy level, which can be explained by the fact that deeper level acceptor defects could not longer be sufficiently ionized.[24,30]

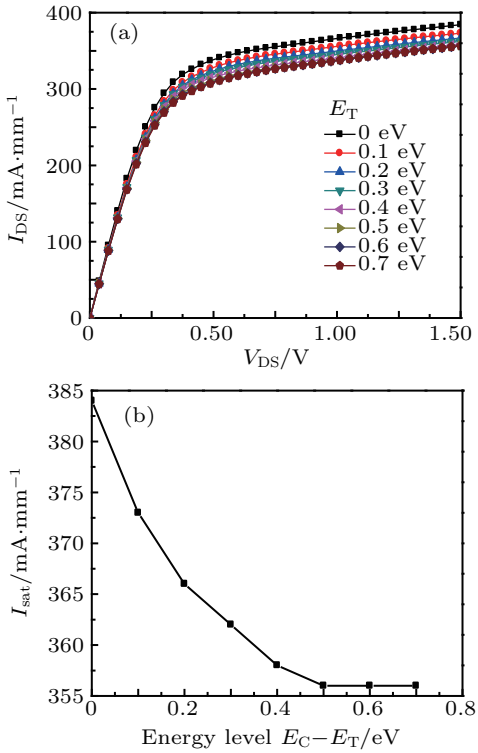


Fig. 5. The effect of E_T on output characteristics. (a) Output current at $V_{GS} = 0$ V; (b) drain saturation current at $V_{DS} = 1.5$ V.

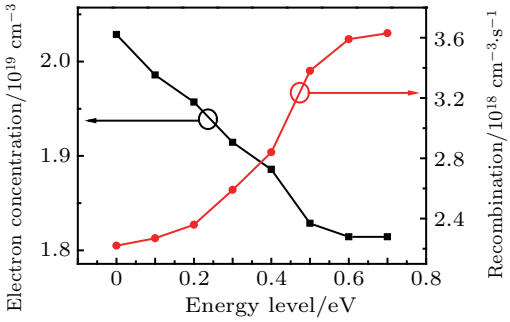


Fig. 6. The electron concentration and recombination rate at the channel of device with different defects energy levels.

As the proton fluence increases, As acceptor defects in greater numbers are necessarily induced in device structure by displacement effect. To explore the impact of induced defect-concentration on InP-based HEMTs, the output channel current and transfer characteristics of InP-based HEMTs are simulated with incident proton voltage of 75 keV and fluence varying from 0 to 4×10^{12} cm^{-2}, as shown in Fig. 7. Both the channel current under V_{GS} of 0 V and transconductance under V_{DS} of 1.5 V demonstrate a decline trend with the increase of proton fluence. The electron concentration in the channel along the vertical direction of the device is plotted with different proton fluences in Fig. 8, which decreases with the increase of the proton fluence. This conforms the fact that the negatively charged As acceptor-like defects induced by proton irradiation capture the free electrons and lead to the decrease of the electron density in the channel region.

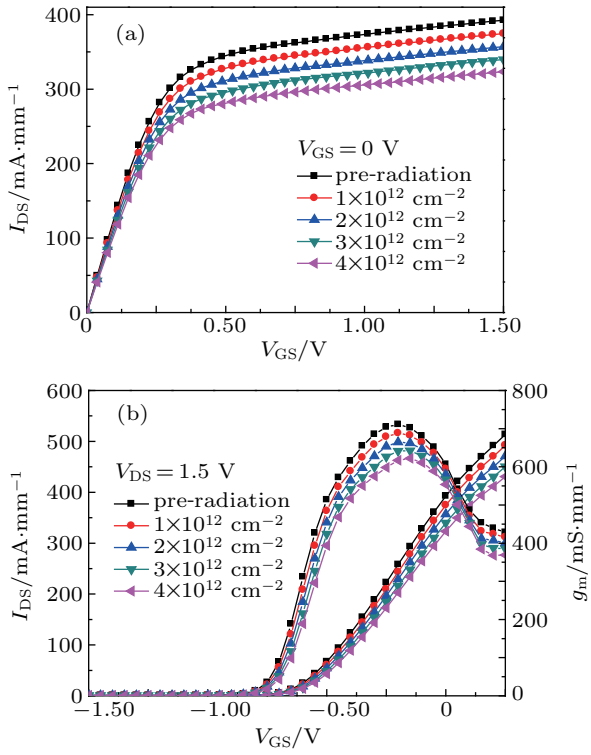


Fig. 7. Characteristics of InP-based HEMTs at different proton fluences. (a) Output channel current; (b) transfer characteristics.

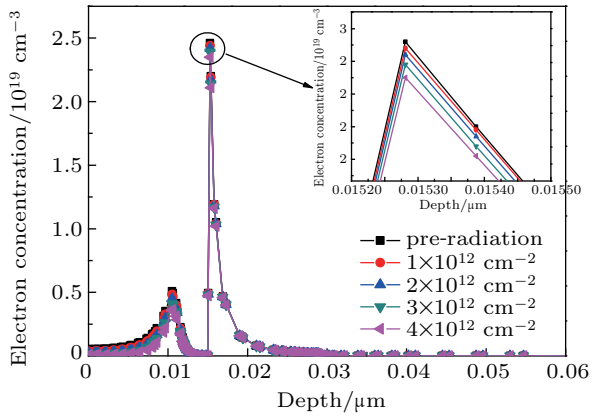


Fig. 8. The electron concentration in InP-based HEMTs with proton fluence from 1×10^{12} cm^{-2} to 4×10^{12} cm^{-2}.

4. Conclusion

In summary, the effect of induced defect on device characteristics of InP-based HEMT is investigated by numerical simulation. The results show that only the acceptor-like defects will influence the device performance. Meanwhile, the drain current gradually decreases with the increase of defect energy level, which ultimately reaches a saturation value with E_T above 0.5 eV. The drain current and transconductance demonstrate obvious decline trend as the proton fluence increases, which is mainly due to the decrease of 2DEG in the channel region induced by As acceptor-like defects.

Acknowledgments

The authors would like to express heartfelt thanks to Huijuan Yao from Xidian University and Lu Zeying from Institute of Electronics of Chinese Academy of Sciences in China for guidance in the operation software.

References

[1] Shangguan L, Ma L H, Li M K, Peng W, Zhong Y H, Su Y F and Duan Z Y 2018 *J. Phys. D: Appl. Phys.* **51** 185603
[2] Wang W, Su Y F, Liu C R, Li D X, Wang P and Duan Z Y 2015 *Chin. Phys. Lett.* **32** 128102
[3] Ma L H, Han W H, Zhao X S, Cao Y Y, Dou Y M and Yang F H 2018 *Chin. Phys. B* **27** 088106
[4] Del Alamo J A 2011 *Nature* **479** 317
[5] Mateos J, Rodilla H, Vasallo B G and González T 2015 *J. Comput. Electron.* **14** 72
[6] Chen J, Zhang Z Y, Zhu M, Xu J T and Li X Y 2017 *Nanoscale Res. Lett.* **12** 33
[7] Wang Y, Sheng X Z, Guo Q L, Li X L, Wang S F, Fu G S, Mazur Y I, Maidaniuk Y, Ware M E, Salamo G J, Liang B L and Huffaker D L 2017 *Nanoscale Res. Lett.* **12** 229
[8] Ajayan J, Ravichandran T, Prajoon P, Pravin J C and Nirmal D 2018 *J. Comput. Electron.* **17** 265
[9] Mei X B, Yoshida W, Lange M, Lee J, Zhou J, Liu P H, Leong K, Zamora A, Padilla J, Sarkozy S, Lai R and Deal W R 2015 *IEEE Electron Device Lett.* **36** 327
[10] Ajayan J and Nirmal D 2016 *Superlattices Microstruct.* **100** 526
[11] Jo H B, Baek J M, Yun D Y, Son S W, Lee J H, Kim T W, Kim D H, Tsutsumi T, Sugiyama H and Matsuzaki H 2018 *IEEE Electron Device Lett.* **39** 1640
[12] Takahashi T, Kawano Y, Makiyama K, Shiba S, Sato M, Nakasha Y and Hara N 2017 *IEEE Trans. Electron Device* **64** 89
[13] Kumar A, Jalota S and Gupta R 2012 *Adv. Space Res.* **49** 1691
[14] Lee I H, Lee C, Choi B K, Yun Y and Chang Y J 2018 *J. Korean Phys. Soc.* **72** 920
[15] Kim H Y, Lo C F, Liu L, Ren F, Kim J and Pearton S J 2012 *Appl. Phys. Lett.* **100** 012107
[16] Rossetto I, Rampazzo F, Gerardin F, Meneghini M, Bagatin M, Zanandrea A, Dua C, di Forte-Poisson M A, Aubry R, Oualli M, Delage S L, Paccagnella A, Meneghesso G and Zanoni E 2015 *Solid State Electron.* **113** 15
[17] Sun S X, Chang M M, Zhang C, Cheng C, Li Y X, Zhong Y H, Ding D, Jin Z and Wei Z C 2018 *Phys. Status Solidi RRL* **12** 1800027
[18] Ratti L, Manghisoni M, Oberti E, Re V, Speziali V, Traversi G, Fallica G and Modica R 2005 *IEEE Trans. Nucl. Sci.* **52** 1040
[19] Wang B, Zhao Y W, Dong Z Y, Deng A H, Miao S S and Yang J 2007 *Acta Phys. Sin.* **56** 1603 (in Chinese)
[20] Zhong Y H, Wang W B, Sun S X, Ding P and Jin Z 2017 *Phys. Status Solidi A* **214** 1700411
[21] Zhong Y H, Yang J, Li X J, Ding P and Jin Z 2015 *J. Korean Phys. Soc.* **66** 1020
[22] Patrick E, Law M, Liu L, Cuervo C V, Xi Y Y, Ren F and Pearton S J 2013 *IEEE Trans. Nucl. Sci.* **60** 4103
[23] Liu M, Zhang Y M, Lü H L and Zhang Y M 2016 *J. Semicond.* **37** 114005
[24] Ge M, Cai Q, Zhang B H, Chen D J, Hu L Q, Xue J J, Lu H, Zhang R and Zheng Y D 2018 *Phys. Status Solidi A* **215** 1700368
[25] Hafsi B, Boubaker A, Ismaïl N, Kalboussi A and Lmimouni K 2015 *J. Korean Phys. Soc.* **67** 1201
[26] Jayakumar G D and Srinivasan R 2017 *J. Comput. Electron.* **16** 307
[27] Sun S X, Ji H F, Yao H J, Li S, Jin Z, Ding P and Zhong Y H 2016 *Chin. Phys. B* **25** 108501
[28] Sun S X, Ma L H, Cheng C, Zhang C, Zhong Y H, Li Y X, Ding P and Jin Z 2017 *Phys. Status Solidi A* **214** 1700322
[29] Liu M, Zhang Y M, Lu H L, Zhang Y M, Zhang J C and Ren X T 2015 *Solid State Electron.* **109** 52
[30] Zhang Z, Cardwell D, Sasikumar A, Kyle E C H, Chen J, Zhang E X, Fleetwood D M, Schrimpf R D, Speck J S, Arehart A R and Ringel S A 2016 *J. Appl. Phys.* **119** 165704